Evaluation of bread dough aeration during kneading by an air-jet impulse system

Niveditha Asaithambi, Joran Fontaine, Eloïse Lancelot, Adrien Rebillard, Dominique Della Valle, Anthony Ogé, José Chéio, Chidanand Duggonahally Veeresh, Alain Le-Bail

EVALUATION OF BREAD DOUGH AERATION DURING KNEADING BY AN AIR-JET IMPULSE SYSTEM

Niveditha ASAITHAMBI[a,b,c], Joran FONTAINE[b,c,d], Eloïse LANCELOT[b,c], Adrien Rebillard[b,c,d], Dominique DELLA VALLE[b], Anthony OGE[b,c], José CHÉIO[d], Chidanand DUGGONAHALLY VEERESH[a] , Alain LE-BAIL[b,c]

[a] Indian Institute of Food Processing Technology, Pudukkottai Road, Thanjavur, Tamil Nadu 613005 – India

[b] ONIRIS, rue de la Géraudière, CS 82225, 44322 NANTES CEDEX 3, (France)

[c] GEPEA, UMR CNRS 6144, ONIRIS, rue de la Géraudière, CS 82225, 44322 NANTES CEDEX 3, (France)

[d] VMI (Vendée Mécanique Industrie), 70 Rue Anne de Bretagne, PA Marches de Bretagne, Saint-Hilaire-de-Loulay, Montaigu Vendée 85600 (France)

Corresponding author : Dominique Della Valle dominique.dellavalle@oniris-nantes.fr

Abstract:

This paper presents a novel system able to determine in touchless conditions some rheological properties of bread dough, by application of a force driven by a short air-jet impulse, and the concomitant surface displacement measurement by a laser interferometer. In this work, it is shown that in the FPD[1] (Food Puff Device) is based on the displacement measurement due to an air jet by a laser interferometer test , a "softening" of the bread dough along the kneading process is observed, although it is well known that the bread dough gets strengthened by the kneading. This paradox is explained by the fact that, during the kneading, not only the dough become smooth and elastic, but a certain air amount is incorporated in the form of small air bubbles. FPD provides an empirical short time rheology test exciting the time scales linked to the air bubbles entrapped in the dough, so that the surface displacement is mainly due to the dough aeration. Demonstrating a good sensitivity to the air content, the FPD test seems a relevant method to follow the kneading process, in the aim of developing a tractable and efficient supervision tool. The bulk properties of the dough are also measured by a conventional creep recovery test in a rotational rheometer. An attempt of modelling the viscoelastic behavior in FPD treated like a creep-recovery test is proposed here, to provide some insights in the baking monitoring.

[1] FPD : Food Puff Device

Keywords: *bread dough mixing, creep-recovery test, porosity, kneading process, laser displacement interferometer*

Highlights:

- FPD (Food Puff Device) is based on the displacement measurement due to an air jet by a laser interferometer
- This exploratory study of the FPD shows feasibility for bread dough monitoring
- First results showed that the FPD is adapted for in-line or on-line control of bread dough aeration during kneading
- A Generalized Kelvin-Voigt system is used to model the dough creep-recovery test induced by the air-jet

1. Introduction

Bread-making consists in processing a mixture of flour, water, salt, yeast and other ingredients, according to four operations: mixing, shaping, proofing, and baking. The mixing step, also named kneading, is the most crucial step regarding to the physical, chemical and physicochemical transformations, detailed in numerous papers of the literature (Schiedt et al., 2013; Tsen and Bushuk, 1963), that are decisive for the subsequent operations and the quality of the final product. The two main objectives of this operation, beyond the simple homogenization of the ingredients, are:

- the hydration of gluten proteins, allowing the formation of a continuous viscoelastic network, determining the gas holding capacity during fermentation and baking (Bloksma, 1990),
- the air intake, in the form of small bubbles. This phenomenon is of key importance, as these bubbles provide nucleation sites in the dough for the further proofing, and so have a major impact on the final cellular structure of the cooked bread loaf.

The assessment of the end of mixing is a very expert decision taken by the baker: it is based on the dough surface smoothness and on the ability of the dough to form a thin film underhand manipulation and stretching, both reflecting the gluten network cohesiveness. An

alternative way to assess the optimum achievement of the kneading is based on the record of the power consumed by the mixer that increases towards a maximum defining the "time to peak", namely t_{PEAK} (Sadot et al., 2017). Beyond t_{PEAK}, the power declines, indicating that any extra mechanical energy is weakening the protein network Figure 1. The air intake leading to the porous structure is highly correlated with the dough structuration, as it increases till t_{PEAK}, after which it saturates or decreases (Sadot et al., 2017). The "baker's optimum time" and the "time to peak" are usually very close (Belton, 2003).

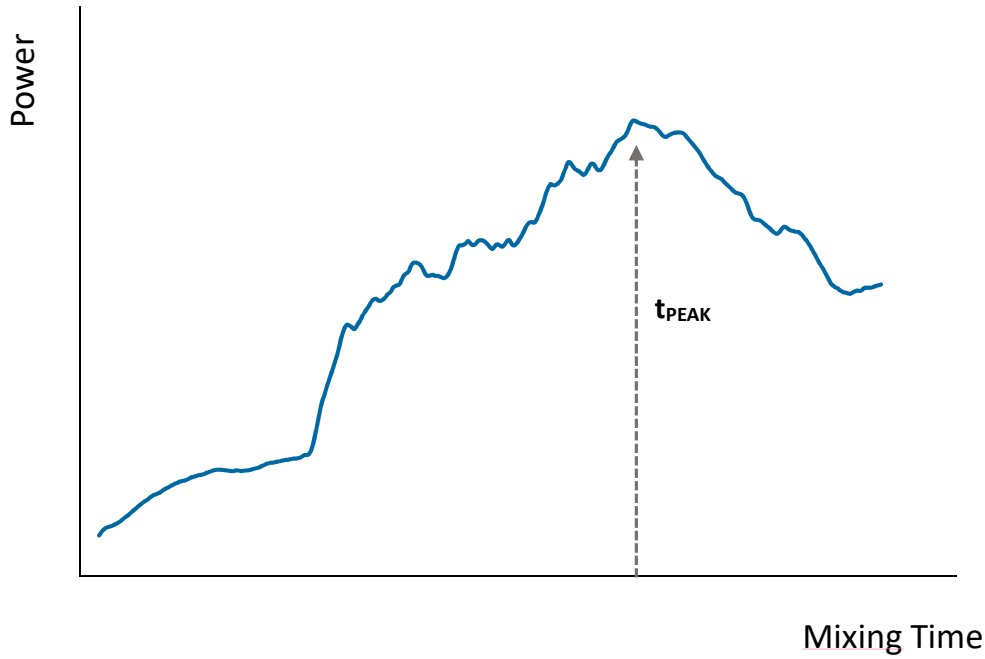

Figure 1: Evolution of the power curve during mixing with the maximum mentioned as t_{PEAK}

The present work aims to study a novel system, the FPD (Food Puff Device), for characterizing the dough evolution during the kneading, and possibly providing a criterion of a "satisfactory" structure of the dough, depending on the baking application, that could be integrated in a supervision system for the sake of industrial dough quality control.

The FPD allows the user to characterize the rheological behavior of food materials by creating deformation over a surface and capturing it by using a displacement transducer based on laser interferometry. The working principle, as well as design aspects, were firstly described by Prussia

74 *et al* (Prussia, Astleford, Hewlett, & Hung, 1994). The device has been proven to be effective in
75 various food products, especially fruit texture: firmness test of peach, kiwifruits and apricot,
76 etc… (Hung et al., 1999; McGlone and Jordan, 2000). Other researches were done in monitoring
77 milk coagulation (Bamelis and De Baerdemaeker, 2006), predicting tenderness of broiler breast
78 meat (Lee et al., 2008), characterizing rheological properties of mayonnaise (Stefan and
79 Kocevski, 2013) and recently on comparing rheological properties of different viscous products
80 (Morren et al., 2015).

81 However, the application to the bread dough seems innovative as no published research work has
82 been identified to our knowledge. This exploratory study aims to characterize the FPD
83 performance for tracking the dough rheology, in conditions where the compliance is a signature
84 for the air content; as seen here before, it can be considered as an alternative parameter for the
85 detection of the kneading achievement. For this, a kneading process was carried out on a
86 reference recipe, and dough samples were collected at different times to be submitted to the FPD
87 test. On the same samples, aeration rate was measured by a weighting method. Meanwhile the
88 bulk rheological properties were controlled by a conventional creep-recovery in a rotational
89 rheometer.

90 The outlines of this paper are as follows: in section 2 the experimental FPD system is presented,
91 as well as the set of devices and methods that were used in the study. The results are presented in
92 section 3, especially the most important feature for practical purpose which is the correlation
93 between the raw measurements of the maximum depth given by the FPD, and the dough aeration
94 rate (or porosity). Additionally, in order to obtain more specific rheological parameters, an
95 attempt of viscoelastic modelling is also presented, by accounting for the evolution of the surface
96 displacement after the air impulse, besides the maximum depth. Under some crude assumptions,
97 the FPD test can provide quantitative values of moduli and time scales, and their evolution at
98 various stages of kneading. Finally, a brief discussion on the efficiency of this system and on
99 further studies that would be necessary to render the system operational is proposed in section 4.

100

101 **2. Materials and Methods**

102 **2.1 Dough formulation**

The three basic ingredients used in the preparation of dough are wheat flour, salt and water. For the reference recipe used in this study, the wheat flour is of Type 55, provided by the Minoterie Girardeau, France. The flour has been analyzed by Upscience France and contained 13.92 % of water, 68.1 % of starch, 12.98 %/dry matter of proteins, 0.51 % of ash content and a falling index of 411 s. Initially, the wheat flour was stored at -20 °C in cold room to prevent any quality change over the experimental duration (4 months). The flour temperature is brought to +4 °C and equilibrated at room temperature. Before mixing, all the ingredients are weighed (Table 1), and a kind of baker's empirical rule is respected with the sum of room, flour and water temperatures equal to 55 °C for all the runs.

Table 1: Formulation of the bread dough

Sl. No	Ingredients	Weight(g)	Flour based %	Mass (%)	Temperature
1.	Flour	3090.2	100.0	61.8	20.2
2.	Water	1854.1	60.0	37.1	14.3
3.	Salt	55.6	1.8	1.1	20.5
Total		**5000**	**161.8**	**100**	**55**

2.2 Kneading device and process

Kneading is carried out in a spiral mixer (SPI11, VMI, Montaigu Vendée, France), whose total volume is 10 L for a 5 kg dough batch. The mixer consists of a spiral tool and a rotating bowl, which induces a planetary motion of the tool to allow the sweeping of the entire volume of dough, as shown in Figure 2. Temperature is monitored by a sensor attached in a pivot, and the tool power is recorded for the determination of the "time to peak" t_{PEAK}, at the maximum consumed power. When the mixer was operated without any stop, the optimum mixed dough was obtained at 270 ± 10 s from the beginning of the kneading.

It is important to notice that before the mixing step, a premixing at low rotation speed is required, in order to homogenize the ingredients. In our study, the premixing was carried out at 100 rpm for the tool and 10 rpm for the co-rotating bowl during 120 s, for obtaining a uniformly mixed dough. The kneading was performed at 200 rpm for the tool and 20 rpm for the bowl. The overall

126 mixing time was 600 s, including the pre-mixing, leading to intentionally overmixed dough, so
127 that sampling may include under mixed, over mixed and optimally mixed conditions.

128

129

130 **Figure 2:** Image of the kneading system, including the rotating bowl and the spiral tool. The
131 pivot is aimed to minimize the power input. The downward motion of the spiral tool is
132 responsible for the air intake.

133

134 **2.3 Sampling method**

135 Sampling was done at regular intervals of 105 s, so that samples are extracted at 5 time marks
136 during the mixing process. Outstanding care was given not to deform the dough samples as
137 manipulations could destroy their natural structure. For the puff test, the dough samples were
138 taken by using a square cookie cutter with a dimension of 40 x 40 x 20 mm. Structure alteration
139 due to the cutting is limited to the edges, and the center is free of any deformation. This protocol
140 also ensures the repeatability of the measurements.

141 For rheometer and porosity, the dough was sampled by using a cylinder of 2.5 cm of diameter.
142 The analysis were done on fresh dough, immediately after mixing, except for the rheometer test
143 for which dough samples were packed in airtight bags, then frozen under -20 °C for time-deferred
144 analysis. It is has been shown that freezing could have an impact on dough rheology especially a
145 weakening of the dough, a decrease in gas retention capacity and a reduced yeast activity (Y.
146 Inoue et W. Bushuk, 1991). However, our study concerns only the mixing step and no yeast has
147 been added to the recipe. In our study, the kinetic of the freezing was rather slow so that the

damage impact is minimized. Moreover, all the samples are subjected to the same potential alterations so that the measurements remain comparable.

2.4 Porosity measurement

The porosity, or void fraction, is determined through the dough current apparent density ρ. For this measurement, a double weighting system based on Archimedes principle was used, following the procedure described by Sadot *et al.* (2017). By knowing the dough density ρ_0, the porosity ϕ is computed by:

$$\phi = 1 - \frac{\rho}{\rho_0} \qquad \text{Equation 1}$$

2.5 Food Puff Device (FPD)

The puff device prototype developed in Oniris consists of an air nozzle combined with a laser displacement transducer (LDT), as seen in Figure 3 The air jet flowing out the nozzle is created by the upflow pressure, and its impact induces a displacement on the dough surface. This displacement is recorded as function of time in a software, with an acquisition rate of 1000 Hz. An exemple of the surface monitoring along 7 s is given in Figure 4 a), where z_{min} denotes the maximum depth of the surface displacement from its initial position, and z_{max} the irresversible depression left in the dough by the air jet. Note that z values are negative, below the reference plane taken at the initial sample surface. The altitude z of the hole bottom and the corresponding thickness h of the dough below, during the air pulse and some seconds later, are précised in Figure 4 b) and c).

A technical issue is that the nozzle have to be accurately positionned with respect to the dough, in such a way that the laser can capture the exact location of air contact. For an easier calibration at each measurement, a special mechanical piece was developed by 3D printing to target the contact point.

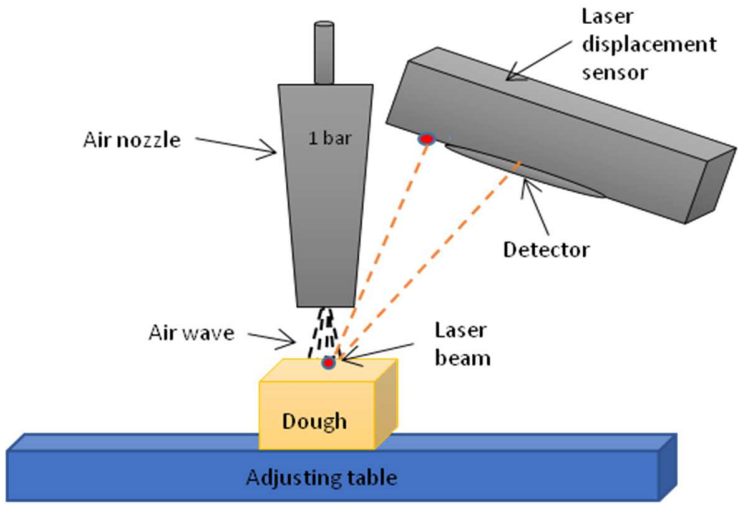

171

172 **Figure 3:** Scheme of the FPD (Food Puff Device)

173

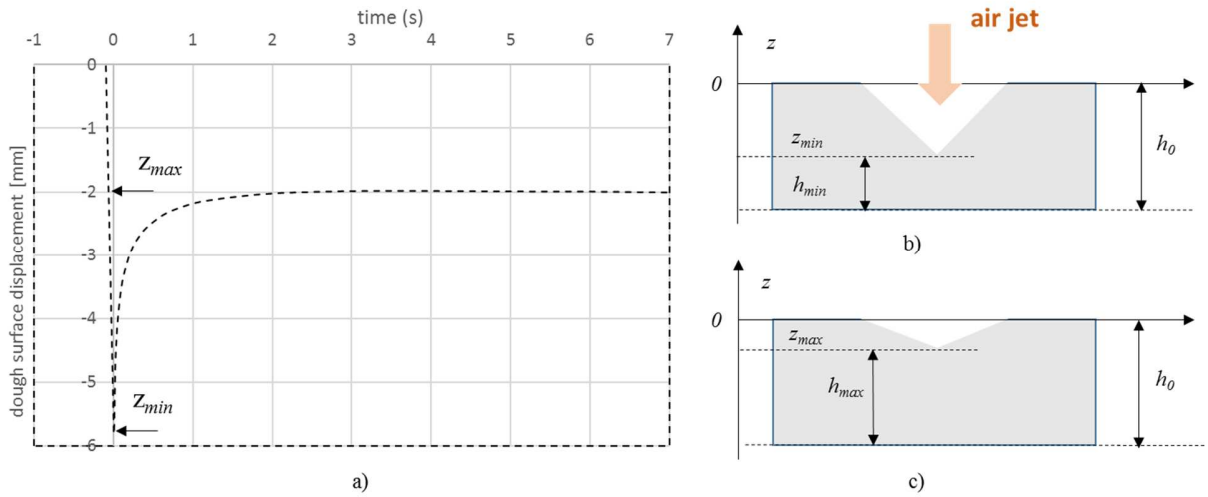

174

175 **Figure 4:** a) Example of a surface displacement monitoring b) dough sample thickness at the end
176 of the air pulse c) dough sample thickness after few seconds from the air pulse.

177

178 **2.6. Modelling the displacement response**

179 The FPD test is similar to a creep-recovery test, as far as a normal stress is maintained by the air-
180 jet during a certain time (about 0.1 s), and then the recovery step is observed from the time that
181 the air-jet ceases. The local displacement at the air jet contact is modelled in order to obtain
182 quantitative information concerning the rheology of the dough, more precisely strain, strain rate,

183 times scales, and the order of magnitude of apparent viscosity and compliance. The purpose is the
184 following:

185 a. compute the normal stress imposed by the air jet impulse,
186 b. compute the elongational strain and strain rate as function of the displacement z at
187 the contact point
188 c. model the dough behavior thanks to a 3 elements Generalized Kelvin-Voigt
189 (3GKV) model,
190 d. identify the rheological constants in the creep–recovery thanks to the experimental
191 response
192

193 a. Estimation of the normal stress induced by the air jet

194 As no experimental method was available for a straightforward measurement during the tests, the
195 output velocity of the jet is estimated by the adiabatic expansion of the air from the pressured
196 tank. The impact force and the normal stress of this jet on the dough surface can be evaluated by
197 Euler's theorem, with the assumption of neglecting the backward air velocity around the jet
198 (much less than the impact component in the cone shaped hole schematized in Figure 4 c).
199 Finally, the normal stress is obtained by dividing the force by the jet diameter. The details of the
200 numerical results are synthetized in Table 2.

201 **Table 2:** Dynamic parameters of the air jet

definition	**variable**	**Value**	**unit**
Up flow absolute pressure	p_i	200, 000	Pa
Nozzle diameter	d	0.003	m
Air mass flowrate	q	0.00277	$kg.s^{-1}$
Air velocity	V	316	$m.s^{-1}$
Impact force	F	0.885	N
Normal stress	σ_0	62, 600	Pa

202

203 b. The strain and strain rate

204 The Hencky strain corresponding to the surface displacement is defined in Equation 7, using the
205 initial sample thickness h_0 and the current one h. The generalization of Figure 4 b) and for a

corresponding z, altitude of the maximum depression at time t, the difference h-z is constant equal to h_0, leading to Equation 3 allowing to compute z from the knowledge of ε.

$$\varepsilon(t) = Ln\left(\frac{h(t)}{h_o}\right) \quad \text{Equation 2}$$

$$z(t) = h_0\left[\exp(\varepsilon(t)) - 1\right] \quad \text{Equation 3}$$

During the very quick air jet impulse, the strain rate is approximated by the ratio of the maximum strain ε_{max} :

$$\dot{\varepsilon}_{max} = \frac{\varepsilon_{max}}{t_0} \quad \text{Equation 4}$$

In the recovery step, the strain rate can be computed from the recording of z as function of time.

c. The 3GKV model

The mechanical model for the linear visco-elastic behavior, shown on Figure 5, is a 3 elements Generalized Kelvin Voigt (3GKV) system, composed of 2 dashpot-spring and 1 dashpot in series, the latter aimed to account for the irreversible deformation after the air pulse. This model is specific for the short time deformations experienced by the dough, and is not comparable with the models encountered in the literature for other rheological tests (Brandner et al., 2018). In this assembly, the creep-recovery can be easily modelled by the sum of the functions for each element. The total deformation during the creep step is expressed by Equation 6, knowing the t_0 value which is of 0.1s in the FPD. The kinetics of the recovery step is described by Equation 7. The constants of the model are the uniaxial elongational moduli (Young moduli) for each element (E_1, E_2), and the retardation times based on the dampers viscosities (θ_1, θ_2), defined in Equation 5.

The linearity of the visco-elastic behavior seems a reasonable assumption in view of the fact that the stress is constant, and the strains vary in a very small range.

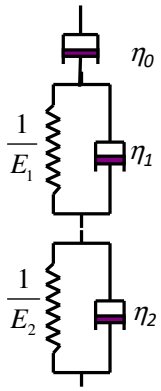

Figure 5 : Mechanical model of the Kelvin-Voigt viscoelastic system

$$\theta_i = \frac{\eta_i}{E_i} \qquad \text{Equation 5}$$

$$\varepsilon_{\max} = -\sigma_0 \left(\frac{1}{E_1}\left(1-\exp\left(-\frac{t_0}{\theta_1}\right)\right)+\frac{1}{E_2}\left(1-\exp\left(-\frac{t_0}{\theta_2}\right)\right)+\frac{t_0}{\eta_0}\right) \qquad \text{Equation 6}$$

$$\varepsilon_{recovery}(t) = -\sigma_0 \left(\frac{1}{E_1}\left(1-\exp\left(-\frac{t_0}{\theta_1}\right)\right)\exp\left(-\frac{t}{\theta_1}\right)+\frac{1}{E_2}\left(1-\exp\left(-\frac{t_0}{\theta_2}\right)\right)\exp\left(-\frac{t}{\theta_2}\right)\right) \qquad \text{Equation 7}$$

d. The response fitting

The experimental response curve over some seconds is computed by fitting the model constants (η_0, E_1, E_2, θ_1, θ_2) thanks to a spreadsheet solver program.

An example of the resulting curve is shown in Figure 6 with the set of constants given in Table 3.

Table 3: Fitting constants of the 3GKV model

variable	value	unit
η_0	2.84 x 10^4	Pa.s
E_1	6.26 x 10^4	Pa
θ_1	3.53 x 10^{-2}	s
E_2	13.05 x 10^4	Pa
θ_2	4.62 x 10^{-1}	s

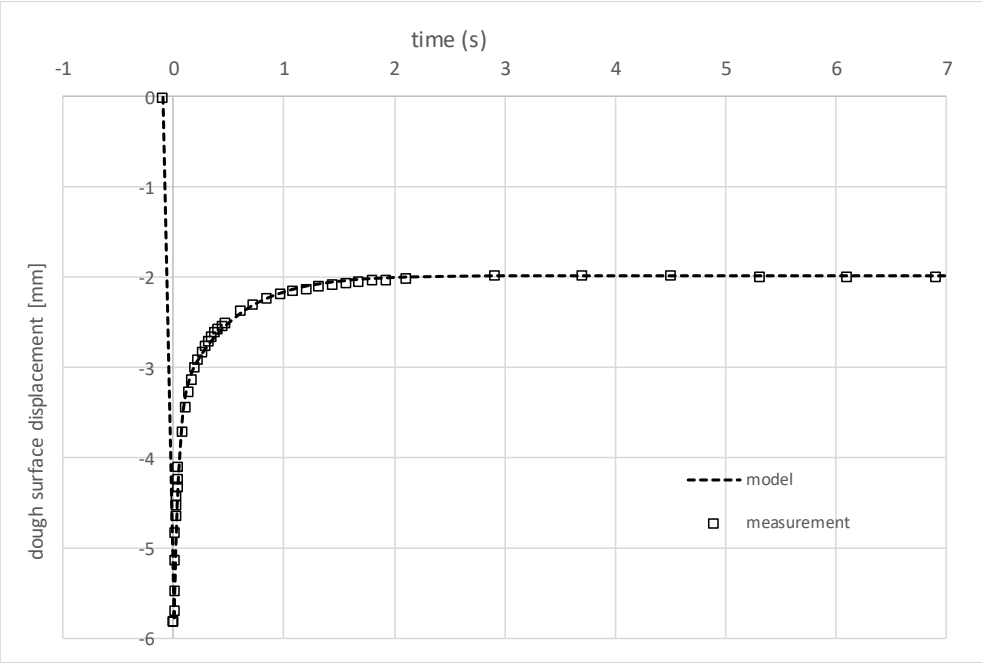

Figure 6 : 3GKV modelling of the surface displacement evolution in FPD

The model constants were determined for all the samples for the same puff stress, so that they provide comparative values to characterize the dough build up.

2.7 Conventional rheometry: creep-recovery in a rotational rheometer

The bulk rheological measurements were carried out in a rotational Rheometer AR 1000 (TA instruments Division de Waters SAS, France). A 40 mm serrated parallel plate geometry was used with a gap of 1 mm. The sample taken out from the cold room is equilibrated to room temperature for 30 mn. The temperature of the bottom plate was maintained at 30 °C by Peltier effect. The surplus materials between the parallel plates were trimmed, and the sides were coated with paraffin oil to prevent drying and oxidation.

In order to compare the trends with the FPD, the creep phase is modelled with and optimized KV model, resulting in the same viscoelastic assembly 3GKV than for the FPD analysis. This means that the fitting is not possible with less than 2 characteristic times, and no accuracy gain is observed with 3 time scales. A pure viscous element is also needed as seen in Figure 7. The same set of rheological constants is used than in section 2.5.1, excepted the moduli that are named G_i to remind that the test is performed in pure shearing. In the recovery time function given in Equation 9, t_c denotes the creep duration.

$$\varepsilon_{creep}(t) = -\tau_0\left(\frac{1}{G_1}\left(1-\exp\left(-\frac{t}{\theta_1}\right)\right)+\frac{1}{G_2}\left(1-\exp\left(-\frac{t}{\theta_2}\right)\right)+\frac{t}{\eta_0}\right) \quad \text{Equation 8}$$

$$\varepsilon_{recovery}(t) = -\tau_0\left(\frac{1}{G_1}\left(1-\exp\left(-\frac{t_c}{\theta_1}\right)\right)\exp\left(-\frac{t}{\theta_1}\right)+\frac{1}{G_2}\left(1-\exp\left(-\frac{t_c}{\theta_2}\right)\right)\exp\left(-\frac{t}{\theta_2}\right)\right) \quad \text{Equation 9}$$

A typical response of the creep-recovery in the rheometer is presented in Figure 7, for a shear stress of 10 Pa and a creep duration of 3mn. The main observation is that the perfect creep prediction with the typical set of data given in Table 4, does not fit correctly the recovery stage, which would be the minimum required to comply with a linear viscoelastic behavior. The reason is that, with bread dough, long time rheology tests are not fully appropriate: the transformations of the dough by various physico-chemical reactions, mainly affecting the disulfide bounds, take place in a few minutes especially under shear, and deeply affect the rheology. That is why in the following modelling, only the creep stage is accounted for to catch the dough behavior in a still "intact" state.

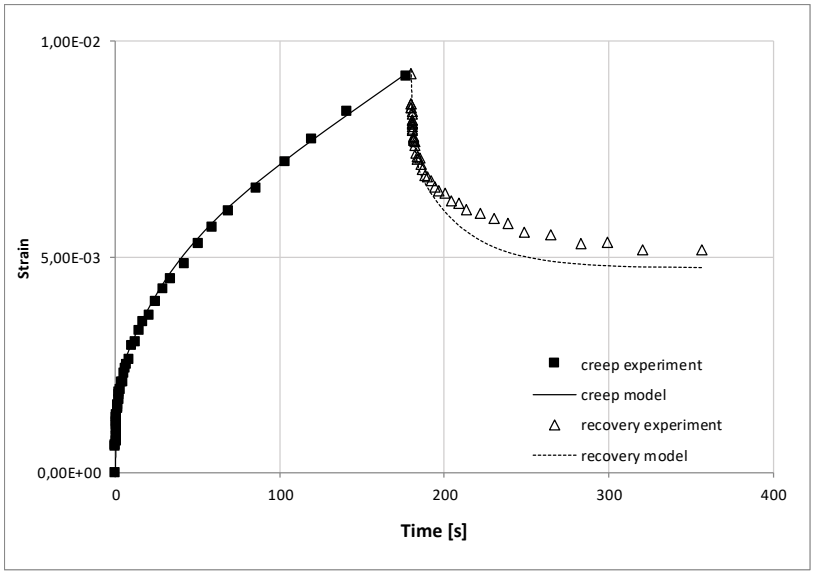

Figure 7 : Example of creep-recovery test for a dough sample in the rheometer

Table 4: Example of fitting constants of the 3GKV model in the recovery test

variable	value	unit

η_0	3.80×10^5	Pa.s
G_1	2.56×10^5	Pa
θ_1	3.59×10^{-2}	s
G_2	2.05×10^5	Pa
θ_2	3.31×10^{-1}	s

2.8. Repeatability and reproducibility

The sampling method described in section 2.3 has been applied to 7 samples from a same batch at each time mark, and for 5 different batches of the same formulation and operating conditions. The experimental data, which are hence averaged on 35 trials for each time mark, are presented with a standard deviation that includes both repeatability and reproducibility. We can infer that for future in-line measurements, the device will need several FPD records to check that the production meets the requirements, given the great variability of the dough.

3. Results and discussion

In this section, the sensitivity of the FPD sensor is determined by comparing the maximum surface depression with the porosity. The rheological properties obtained by FPD and rheometry, in the conditions described in section 2, are analyzed to bring to light control parameters for the different aspects of the dough evolution during the kneading.

3.1 Evolution of power curve and determination of the optimum mixing time

The tool power and the temperature over mixing time are displayed in Figure 8. The power needed for optimum dough development is marked as a peak around 500 s, with a time line origin at the beginning of the pre-mixing and including the interruptions, and that are numbered from 1 to 5 to reference the time marks.

The temperature of the dough increases with the mixing time, mainly due to the heat generated by the frictional force. A certain heat sink can be attributable to the dissolution of flour in the water, but remains negligible in the temperature evolution. The maximum acceptable final temperature of the dough is found out to be 27 °C, above which the dough becomes sticky.

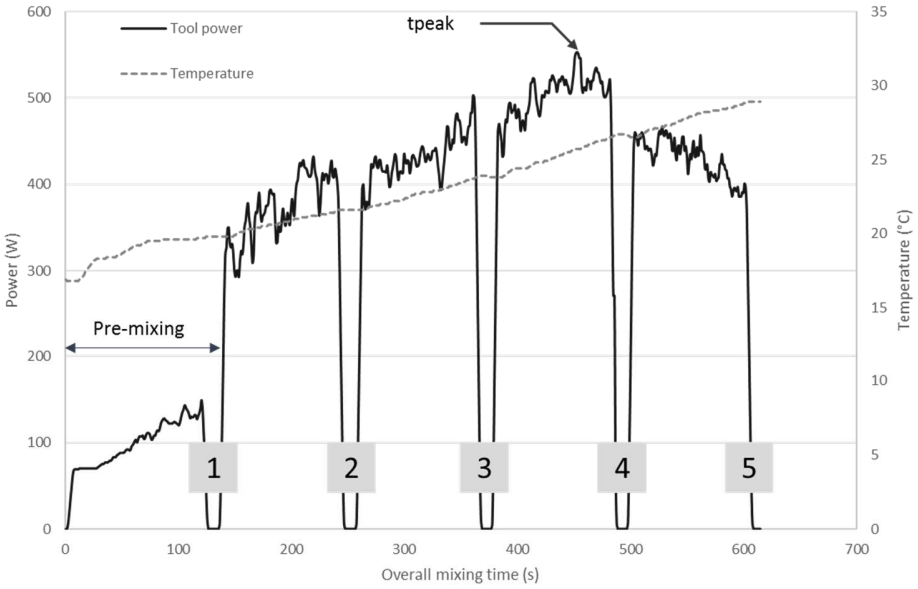

Figure 8 : Typical evolution of the power and temperature with mixing time, identification of the optimum mixing time or "time to peak" t_{PEAK}. The gaps in the curve correspond to stoppages for the sampling.

3.2 Tracking the porosity by FPD measurements

In the following evolution graphs, the time is counted as from the beginning of the mixing end of the pre-mixing and apart from the sampling stoppages. The evolution of respectively the maximum depth measured by the FPD and the porosity is presented in Figure 9 and Figure 10. It can be observed that both curves present an extremum at t_{PEAK}. When plotting the porosity as function of the maximum depth, a linear relationship between these two parameters arises, as assessed by the exponent 1 of the power law fitting curve. Especially, the time mark 5 corresponding to overmixed conditions is consistent with the trend curve, with a lower air content than for the time mark 4 at t_{PEAK}. This result is very promising, as it means that the same relative uncertainty is expected on the porosity than on the FPD measurement for the monitoring.

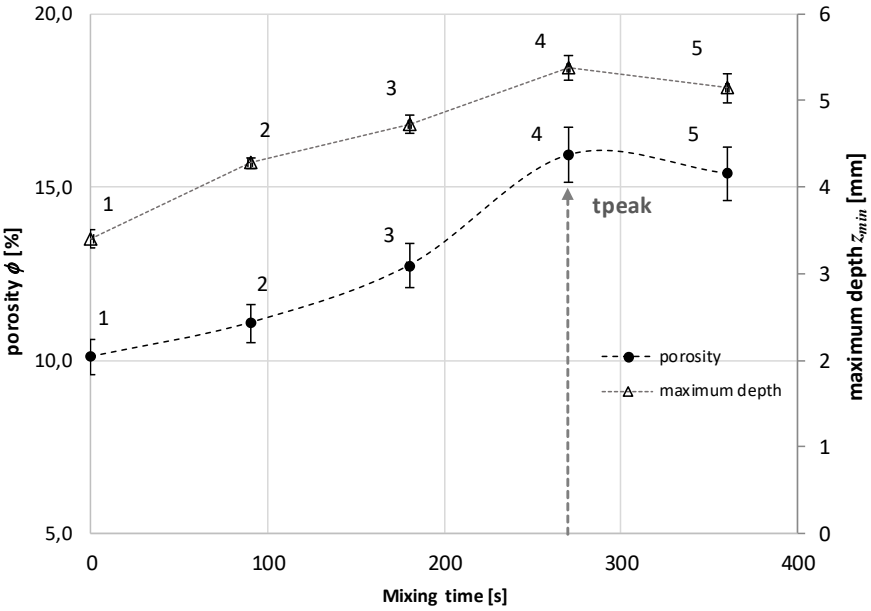

315

316 **Figure 9 :** Evolution of the maximum depth and the porosity (%) with the mixing time (s)

317

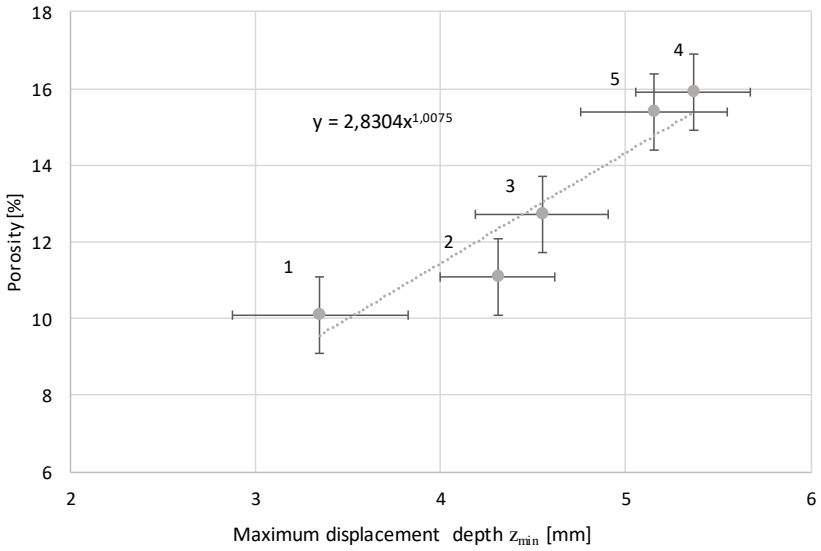

318

319 **Figure 10 :** Porosity as function of the maximum depth

320 **3.3 Rheological constants from FPD modelling**

321 The experimental displacement fitted by the 3GKV model provides the trend for the model
322 constants at the time marks along the kneading. The global compliance *J*, defined in Equation 10,
323 present a maximum as well as the maximum depth for the time mark 4, while the extensional

viscosity is minimum, meaning that the dough is softer at the "time to peak". The evolution of both parameters during the kneading are presented in Figure 11.

$$J = \frac{1}{E_1} + \frac{1}{E_2} \qquad \text{Equation 10}$$

Figure 13 show that they remain nearly constant during all the kneading process. We suggest some explanations for these time scales. Considering the aerated dough structure, the lowest one should be linked to the gas compressibility, which is of order η_{air}/p, respectively the viscosity of air and the absolute pressure, giving around 10^{-10} s. Such a small time cannot be captured with an acquisition frequency of 10^3 s^{-1}, and moreover the mechanical system (air jet and dough motion) have a certain inertia. The first time scale, θ_1, found about 3 x 10^{-2} s, probably represents one of these response time but doesn't contain any physical meaning. The second retardation time, θ_2, seems more relevant, as is appears to be close of the deformation time of the bubble in a viscous matrix. Actually this deformation time scale t_b can be computed by Equation 11:

$$t_b = \frac{\eta_0 d}{2\sigma} \qquad \text{Equation 11}$$

With a typical set of values, η_0 = 24600 Pa.s at t_{PEAK}, the interfacial tension of order 0,04 $N.m^{-1}$, and the bubbles diameters ranging between 5 and 40 µm (see Figure 13), the deformation time ranges between 1,5 and 12 s. This order of magnitude is fairly targeted by the FPD time scale, given by Equation 12, which is of order 0.5 s at t_{PEAK}. This means that creep-recovery in the FPD is the manifestation of the natural time of the bubbles, while the dough matrix is not or weakly deformed. One can notice that this time scale is independent of the bubble number, conversely of the maximum depth in the FPD that cumulates the deformations of the bubbles present in the volume, and thus is linked to the void fraction.

$$t_{FPD} = \frac{1}{\dot{\varepsilon}_{\max}} \qquad \text{Equation 12}$$

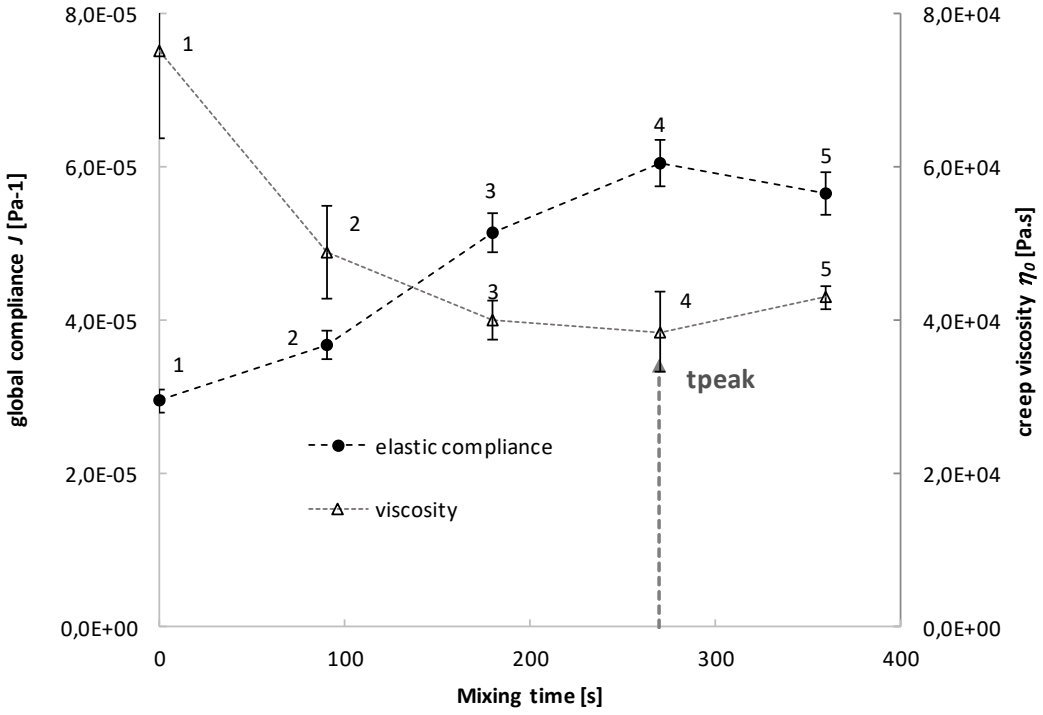

346

347 **Figure 11 :** Evolution of the global compliance and the viscosity of the dough computed by the
348 3GKV model in the FPD

349

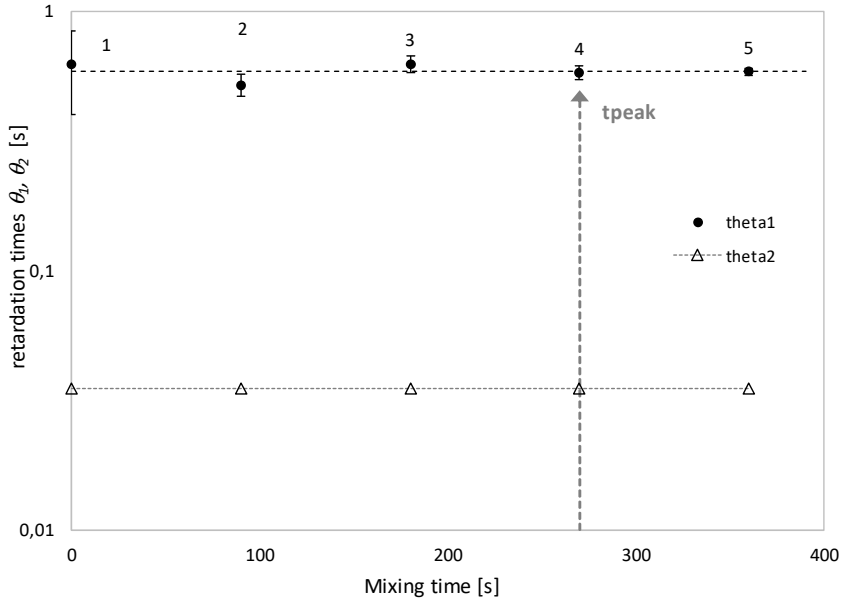

350

351 **Figure 12 :** Evolution of retardation times of the dough computed from the 3GKV model in the
352 FPD

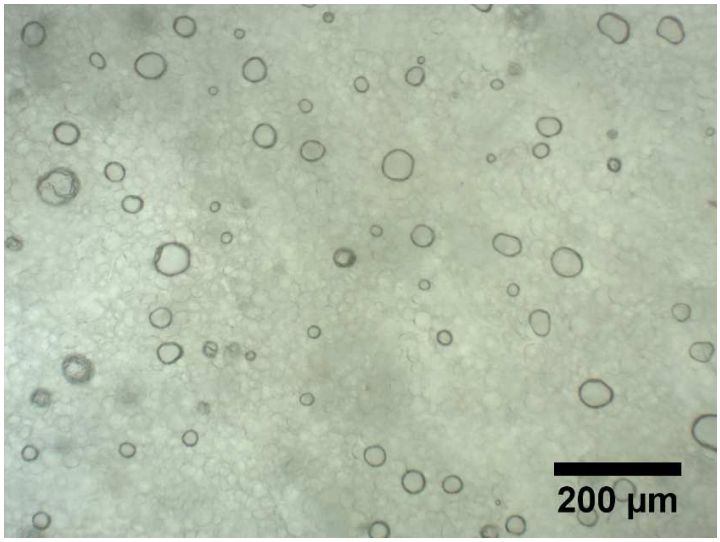

Figure 13 : Aspect of the air bubbles in the dough after kneading from optical microscopy (Digital Image Processing Lab of Oniris)

3.4 Rheological constants from creep-recovery modelling in the rheometer

In a similar purpose than for the FPD, the evolution along the kneading of the fitting constants of the 3GKV model are examined. The evolution of the compliance and the viscosity is presented in Figure 14. A first observation is that the ratio of the standard deviation by the variation range is about 52%: the significance of the rheometer measurements seems by itself relatively low. Nevertheless, the compliance presents a significant decreasing trend, reflecting the gain of stiffness in the mixing process. The increase of the viscosity is consistent with this feature. Considering the first retardation time θ_1 plotted in Figure 15, its value about 2 s keeps quite constant over the kneading, suggesting that it could be a manifestation of the air bubbles, that withstand an elastic deformation under shear. Unfortunately, the system is not sensitive enough to discriminate any variation of the bubble time scale over the mixing, and the comparison with Equation 11 can only be an order of magnitude. It is also likely that lower time scales could exist under this value, exhibited by the FPD, but the creep test is not able to detect them because of its "long" response time. The second time scale varies in the range [25-45] s, and is related to the bulk rheology. This parameter exhibits a maximum for the peak, clearly meaning the optimal

elasticity for the dough at the time mark 4, and loss of elasticity for overmixed dough at the time mark 5.

Providing the rather low sensitivity of the measurements, the rheological behavior exhibited by the rheometer is opposite to the one observed in the FPD; the apparent compliance decreases in creep test, whilst it increases in the FDP. Thus, the creep test results in the rheometer, carried out with the same batch of samples than for the FPD and proving that the dough become stiffer, reinforce the presumption that the air content is primarily responsible of the softening in the FPD.

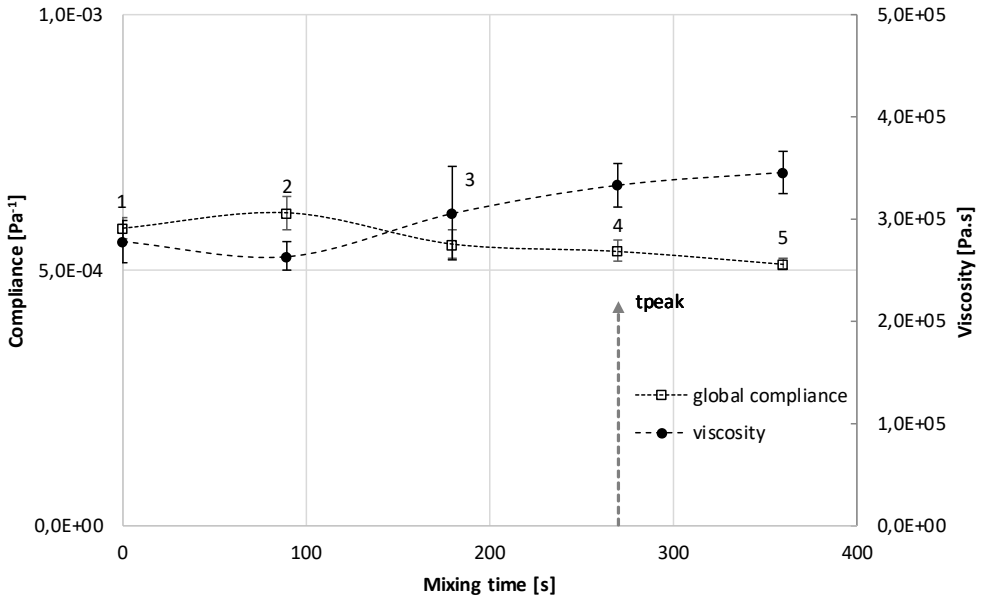

Figure 14 : Evolution of the apparent compliance and viscosity of the dough computed from the 3GKV model in the rheometer creep test

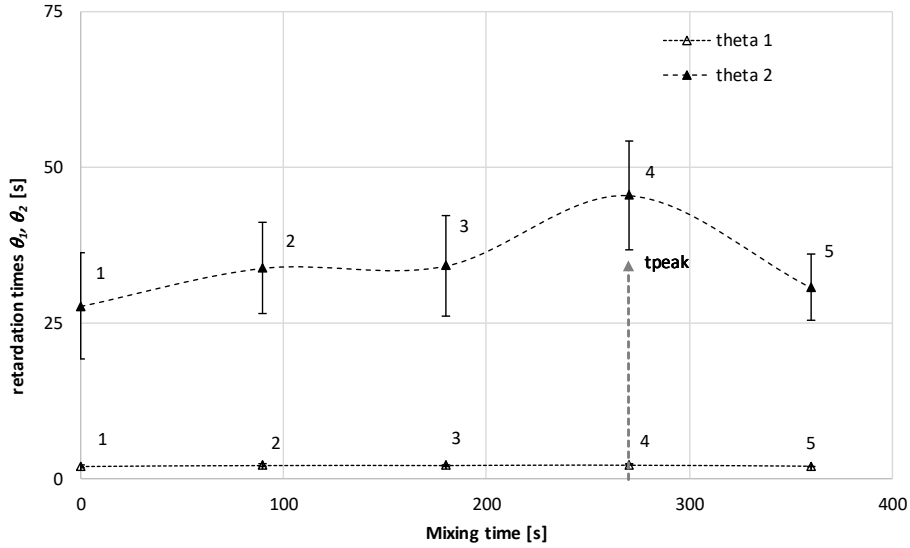

Figure 15 : Evolution of retardation times of the dough computed from the 3GKV model in the rheometer creep test

4. Conclusion

The tracking of the dough build-up during the kneading is a real challenge. An innovative probe has been assessed in this study, based on the impact of an air pulse on the bread dough surface. Such sensor appears as a reliable indicator of the amount of air embedded in the dough. Actually, the maximum depth observed in the test is highly correlated to the air content: a linear relationship was established, for a specific formulation and operating parameters. During mixing, the amount of air entrapped in the dough increases as the dough elasticity progresses. Independent measurements have shown that the maximum air content is reached very close the "time to peak", so that FPD may provide a good indicator for the mixing achievement. With the help of the FPD dough recovery modelling, a characteristic time appeared to be linked to the bubbles compression. A similar time scale arises from a creep test in the rheometer, but also a much longer one, reflecting the elasticity of the dough. The trend for the compliance evolution was found to be opposite in the FPD and in the rheometer, meaning that the first parameter was linked to the air bubbles, and the second to the effect of the bulk elasticity.

In the aim of using the FPD for a full supervision of the kneading in baking factories, some additional knowledge is necessary concerning other formulations, especially the effect of the fat matter that could modify the bubbles interfaces. Moreover, a technical issue must be overcome,

406 with the automation of the probe location at the exact heightening required for the laser to point
407 the center air the air jet. Finally, the study shows that several measurements are necessary to get a
408 reliable information, and for that the probe is supposed to react very rapidly to the supervision
409 command, of course in the limit of the time interval of the air jet (0.1 s), but before any
410 significant change in the dough.

411

412 **Acknowledgments:** This project took place within the MIXI-LAB project funded by the
413 National Agency for Research (ANR – agreement ANR- 15-LCV3-0006-01).

414

415 **5. References**

416 Bamelis, F.R., De Baerdemaeker, J.G., 2006. Use of the Foodtexture Puff Device to monitor milk
417 coagulation. J. Dairy Sci. 89, 29–36. https://doi.org/10.3168/jds.S0022-0302(06)72066-5
418 Belton, P.S., 2003. 13 - The molecular basis of dough rheology, Second Edi. ed, Bread Making:
419 Improving Quality. Woodhead Publishing Limited. https://doi.org/10.1016/B978-1-85573-
420 553-8.50017-4
421 Bloksma, A.H., 1990. Rheology of the Breadmaking Process. Am. Assoc. Cereal Chem. 35, 228–
422 236.
423 Brandner, S., Becker, T., Jekle, M., 2018. Wheat dough imitating artificial dough system based
424 on hydrocolloids and glass beads. J. Food Eng. 223, 144–151.
425 https://doi.org/10.1016/j.jfoodeng.2017.12.014
426 Hung, Y.C., Prussia, S.E., Ezeike, G.O.I., 1999. Nondestructive firmness sensing using a laser
427 air-puff detector. Postharvest Biol. Technol. 16, 15–25. https://doi.org/10.1016/S0925-
428 5214(98)00103-3
429 Lee, Y.S., Owens, C.M., Meullenet, J.F., 2008. A novel laser air puff and shape profile method
430 for predicting tenderness of broiler breast meat. Poult. Sci. 87, 1451–1457.
431 https://doi.org/10.3382/ps.2007-00463
432 McGlone, V.A., Jordan, R.B., 2000. Kiwifruit and apricot firmness measurement by the non-
433 contact laser air-puff method. Postharvest Biol. Technol. 19, 47–54.
434 https://doi.org/10.1016/S0925-5214(00)00068-5

435 Morren, S., Van Dyck, T., Mathijs, F., Luca, S., Cardinaels, R., Moldenaers, P., De Ketelaere, B.,
436 Claes, J., 2015. Applicability of the foodtexture puff device for rheological characterization
437 of viscous food products. J. Texture Stud. 46, 94–104.
438 https://doi.org/https://doi.org/10.1111/jtxs.12118
439 Prussia, S., Astleford, J., Hewlett, B., Hung, Y.-C., 1994. Non-Destructive Firmness Measuring
440 Device. https://doi.org/10.1007/s00253-005-1916-3
441 Sadot, M., Cheio, J., Le-Bail, A., 2017. Impact on dough aeration of pressure change during
442 mixing. J. Food Eng. 195, 150–157. https://doi.org/10.1016/j.jfoodeng.2016.09.008
443 Schiedt, B., Baumann, A., Conde-Petit, B., Vilgis, T.A., 2013. Short- and long-range interactions
444 governing the viscoelastic properties during wheat dough and model dough development. J.
445 Texture Stud. 44, 317–332. https://doi.org/10.1111/jtxs.12027
446 Stefan, K., Kocevski, D., 2013. Determination of the rheological properties of mayonnaise. Int. J.
447 Eng. 4, 8269.
448 Tsen, C.C., Bushuk, W., 1963. Changes in Sulfhydryl and Disulfid Contents of Doughs. Cereal
449 Chem. 40, 399–408.
450
451
452